$^{14}C(p,n)^{14}N$ reaction at $E_p = 35$ MeV

M. Kabasawa, A. Satoh, Y. Takahashi, T. Kawamura, K. Furukawa, and T. Nakagawa
Department of Physics, Tohoku University, Sendai 980, Japan

H. Orihara, T. Niizeki, and K. Ishii
Cyclotron and Radioisotope Center, Tohoku University, Sendai 980, Japan

K. Miura
Tohoku Institute of Technology, Sendai 982, Japan

H. Ohnuma
Department of Physics, Tokyo Institute of Technology, Oh-okayama, Tokyo 152, Japan
(Received 18 July 1991)

Differential cross sections for the $^{14}C(p,n)^{14}N$ reaction were measured at $E_p = 35$ MeV. A number of spin-isospin excitations have been observed including Gamow-Teller-type $0^+ \rightarrow 1^+$ and $0\hbar\omega$ and $1\hbar\omega$ jump stretched transitions. Distorted-wave Born-approximation calculations using shell-model wave functions have successfully reproduced the experimental results. Renormalization factors of about 0.5 were required for the spin-flip transitions leading to the 3.947-MeV 1^+ state and to the 7.026-MeV 2^+ state, where $\Delta J(\Delta L, \Delta S) = 1(0,1)$ and 2(2,1), respectively. Proton and neutron optical-potential parameters were derived in the course of the present work.

PACS number(s): 25.40.Ep

I. INTRODUCTION

The nucleus ^{14}C is a unique one in the p shell having an even number of protons with two extra neutrons, and therefore the (p,n) reaction on ^{14}C provides information on various aspects of isovector structures in this reaction. We have carried out [1–4] a systematic study of (p,n) reactions at 35 MeV to explore spin-isospin excitations in nuclei, including $0^+ \rightarrow 1^+$ transitions corresponding to Gamow-Teller (GT) β-decay, stretched particle-hole excitations, and $0^+ \rightarrow 0^-$ transitions which may be strongly related to one-π exchange in hadron scattering. The $^{14}C(p,n)^{14}N$ reaction contains all these subjects. The 1^+ transition to the 3.947-MeV state in ^{14}N, which corresponds to strong GT β decay, has presented a good yardstick to calibrate (p,n) cross sections against the GT β-decay strength [5]. Another 1^+ transition, that to the ground state of ^{14}N, should be highly hindered unless the $\Delta J(\Delta L, \Delta S) = 1(2,1)$ component and/or higher-order processes contribute to the (p,n) cross section [2], and has long been discussed by many authors [6]. The J^π values of the two states at 6.444 and 8.48 MeV are known to be 3^+ and 4^-, respectively, suggesting that these are stretched particle-hole states of $0\hbar\omega$ $(\pi p_{3/2}, \nu p_{3/2}^{-1})$ and $1\hbar\omega$ $(\pi d_{5/2}, \nu p_{3/2}^{-1})$ character. There is a known 0^- state at $E_x = 4.915$ MeV in ^{14}N, which is a candidate to study the isovector $\Delta J^\pi = 0^-$ transition in addition to that in the $^{16}O(p,n)^{16}F$ reaction [4]. Furthermore, there are no other target nuclei in the p shell where one can observe the isobaric-analog transition corresponding to a pure Fermi β decay. This, together with the 1^+ transition to the 3.947-MeV state, has provided a measure of the isovector non-spin-flip and spin-flip strengths of the central effective interaction [7,8]. Besides these unique features, the (p,n) reaction on ^{14}C may be the only case where both the proton scattering experiment on the target nucleus and the neutron scattering experiment on the residual nucleus are possible. Thus we are able to obtain a comprehensive set of the optical-potential parameters in the isovector channel by analyzing proton and neutron scattering data and the analog transition data.

Shell-model transition amplitudes for p-shell nuclei needed for microscopic distorted-wave Born-approximation (DWBA) calculations are available from the Cohen and Kurath wave functions [9] for the positive-parity states, and from Millener and Kurath wave functions [10] for the negative-parity states. By sampling the (p,n) reactions on ^{12}C and ^{16}O at $E_p = 35$ and 40 MeV, we have examined [11] the reliability of the information obtained from DWBA analyses of the low-energy (p,n) data. The tensor part of the effective nucleon-nucleon interaction, which is crucial in the DWBA prediction, has been separately tested by studying the isovector-type $\Delta J^\pi = 0^-$ transitions in p-shell nuclei [1]. Several 1^+ excitations with the dominant $\Delta J(\Delta L, \Delta S) = 1(2,1)$ components are observed in the $^{34}S(p,n)^{34}Cl$ reaction [2]. They are found to be quenched to less than a half of the predicted strengths. The analyses in these studies show that the effects of higher-order and exchange processes give negligibly small contributions in most cases. It has also been found [2,11] that the use of different distorting potential parameters may introduce an ambiguity of $\sim 20\%$ in the absolute magnitude of predicted cross sections.

In this paper we report the experimental data of the $^{14}C(p,n)^{14}N$ reaction obtained at $E_p = 35$ MeV, and the results of their DWBA analysis.

II. EXPERIMENTAL PROCEDURE

The experiment was performed using a 35 MeV proton beam and the time-of-flight facilities at Cyclotron and Radioisotope Center, Tohoku University. The target was a self-supporting foil of radioactive ^{14}C. Its thickness, 168 $\mu g/cm^2$ in ^{14}C, was determined by comparing the yield of elastically scattered protons with optical model calculations described later. The target was moved up and down during the elastic scattering measurements, and was found to be uniform within $\pm 12\%$. The target was mounted in a small container to prevent radioactive carbon from sputtering and contaminating the scattering chamber. The windows of this small container were covered by 1-mg/cm^2-thick enriched ^{12}C foils. Overall time resolution was typically 1.0 ns corresponding to 120 keV for the most energetic neutron over a flight path of 44.3 m. The detector efficiencies were obtained from Monte Carlo calculations for monoenergetic neutrons with $E_n \leq 34$ MeV. Absolute detector efficiencies were also measured by counting neutrons from the $^7Li(p,n)^7Be$ reaction and comparing its yields with the absolute neutron fluence determined by activation. Errors in the absolute magnitude of the cross sections were estimated to be less than 15%, the dominant part of which was due to the nonuniformity of the target. Experimental details are given in our previous report [12]. Typical neutron spectra taken for the $^{14}C(p,n)^{14}N$ reaction at laboratory angles 25° and 75° are displayed in Figs. 1(a) and (b), respectively. Measured angular distributions of emitted neutrons are shown in Figs. 3 through 8 along with DWBA predictions discussed in the following sections.

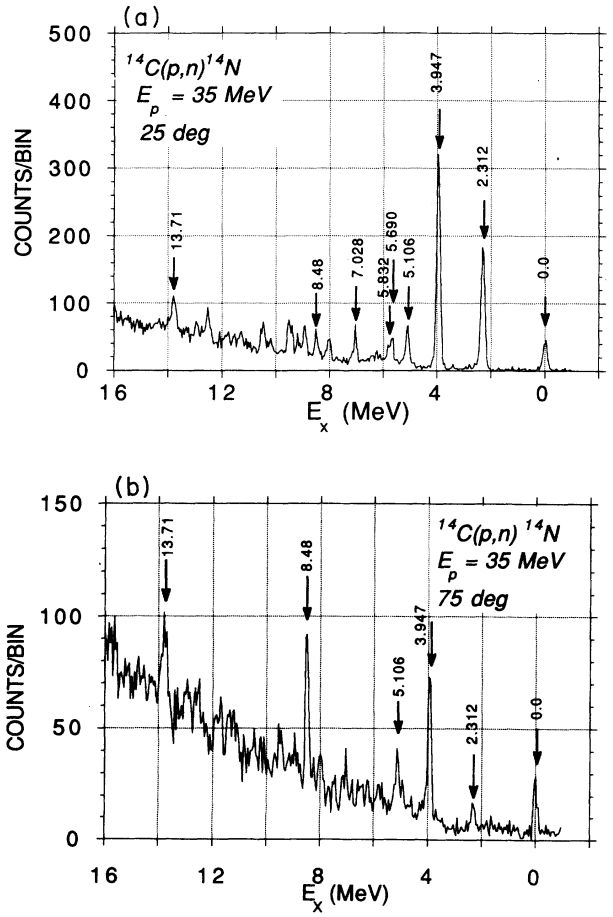

FIG. 1. Sample energy spectra for the $^{14}C(p,n)^{14}N$ reaction taken at laboratory angles (a) 25° and (b) 75° with a flight path of 44.3 m. Energy per bin is 25 keV.

Figure 5(b) also shows the differential cross sections for the $^{14}N(p,n)^{14}O$(g.s.) reaction taken with similar experimental setup. This is the analog to the $^{14}C(p,n)^{14}N$(g.s.) reaction, and these two transitions are expected to be equivalent except for the statistical spin factor and isospin coupling. The corresponding cross sections for the $^{14}C(p,n)^{14}N$(g.s.) reaction are indeed almost three times as large in magnitudes as those for the $^{14}N(p,n)^{14}O$(g.s.) reaction as seen in the figure.

III. OPTICAL POTENTIAL

Appropriate optical potentials are required to generate distorted waves in the DWBA analyses of (p,n) cross sections. The potential parameter sets in both entrance and exit channels can be derived by analyzing elastic scattering data so long as the participant nuclei are stable or have sufficiently long lifetime. In most cases, however, the residual nuclei of (p,n) reactions are unstable. Thus, a global optical-potential parameter set, with which we can derive parameters by interpolation, is required for DWBA calculations. In this regard the $^{14}C(p,n)^{14}N$ reaction is a special case, where nucleon scattering experiments are possible in both channels.

We derived two sets of optical-potential parameters for the present analysis. The first set is due to global search of parameters for the p-shell nuclei, and obtained by fitting the proton and neutron scattering data on ^9Be, $^{12,13}C$, $^{14,15}N$, and ^{16}O. This set was used to determine the ^{14}C target thickness. The second set is that particular to the $A=14$ system, and obtained by simultaneously fitting three data sets, the $^{14}C+p$ and $^{14}N+n$ elastic scattering data and the $^{14}C(p,n)^{14}N$(IAS) quasielastic scattering data. It should be stressed that the $^{14}C(p,n)$ reaction is the only reaction in which one can observe a pure Fermi transition in p-shell nuclei to study the isovector term of an optical potential.

The optical potential is parametrized in terms of standard Woods-Saxon form as

$$U(r)=V_0 f_r(r)+4ia_i W_D \frac{d}{dr} f_i(r) + \left[\frac{\hbar}{m_\pi c}\right]^2 V_{LS}\frac{1}{r}\frac{d}{dr} f_{LS}(r)\mathbf{L}\cdot\boldsymbol{\sigma}+V_C(r)\,,$$

where

$$V_C(r)=\begin{cases}(Ze^2/2R_C)(3-r^2/R_C^2) & (r\leq R_C)\\ Ze^2/r & (r>R_C)\,,\end{cases}$$

and

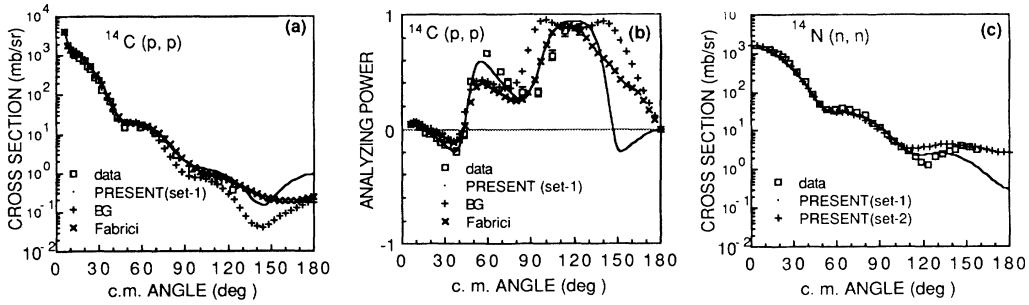

FIG. 2. Optical-model analyses for the (a) cross sections and (b) analyzing powers of 35-MeV protons elastically scattered by ^{14}C. Experimental data were taken from Ref. [18]. Shown in (c) are optical-model analyses for the cross sections of 25-MeV neutrons scattered by ^{14}N. Experimental data were taken from Ref. [22]. See text for the differences between set 1 and set 2.

$$f_i(r)=\left[1+\exp\left[\frac{r-R_i}{a_i}\right]\right]^{-1}.$$

The absorption potential contains only a surface term. This is because the surface diffuseness is relatively large compared to the radius for p-shell nuclei, and the surface absorption is much larger than the volume absorption. We included the volume absorption term in preliminary analysis. However, the volume absorption tended to become very small during the search, and no significance could be attached to its final value. Therefore we left out the volume absorption in later analyses to reduce the fitting parameters. The mass-number dependence of each parameter is included following Myers [13] and Fabrici *et al.* [14]. The diffuseness parameters are assumed to depend on $(N-Z)/A$ following Refs. [15] (BG) and [16], while incident-energy dependence is introduced only for the potential-depth parameters. Among the parameters involved, those of the isovector terms are directly connected to the cross sections of the quasielastic (p,n) reaction studied in the present work.

Parameter search was carried out with programs RELOM [17] and IASEARCH [18]. Elastic scattering data were obtained from Refs. [14,19–21],[22–27] for protons, and Refs. [22,23,28–32] for neutrons. The radius and diffuseness parameters were determined from the elastic scattering data in the first set (hereafter referred to as set 1), and only the depths of the isovector potentials were searched for using the quasielastic data. This was not the case in the second set (set 2), and the geometrical parameters were varied in the simultaneous fit to the (p,p), (n,n), and (p,n) data for the $A=14$ system.

Tables I and II list the obtained parameters of the set-1 and set-2 potentials, respectively, for the proton and neutron. The results for the ^{14}C(p,p) scattering are illustrated in Figs. 2(a) and (b) as representative examples. Calculations with the optical potential parameters by BG and Fabrici *et al.* are also presented for comparison. The BG parameter set was originally obtained by analyzing the elastic data for nuclei heavier than $A=40$, but it has been known to give reasonable fits also to the elastic data for lighter nuclei. As far as the cross section data are concerned, these parameter sets give similarly good descriptions of the data. Analyses of the analyzing-power data, however, exhibit clear differences of the parameter

TABLE I. Optical-potential parameters for the set-1 potential.

		Proton	Neutron
V_0	$42.99+\frac{729.3}{A^2}-0.3(E-35)$	$+17.55\frac{(N-Z)}{A}+0.4\frac{Z}{A^{1/3}}$	$-17.55\frac{(N-Z)}{A}$
r_r		$1.296-\frac{0.906}{A^{2/3}}$	$1.155-\frac{0.344}{A^{2/3}}$
a_r		$0.766-\frac{0.483}{A^{2/3}}-0.221\frac{(N-Z)}{A}$	$1.134-\frac{2.891}{A^{2/3}}$
W_D	$7.127-\frac{176.4}{A^2}+0.01(E-35)$	$+6.40\frac{(N-Z)}{A}-0.01\frac{Z}{A^{1/3}}$	$-6.40\frac{(N-Z)}{A}$
r_i		$1.537-\frac{1.292}{A^{2/3}}$	1.350
a_i		$0.450+\frac{0.356}{A^{2/3}}+0.587\frac{(N-Z)}{A}$	$0.570-\frac{0.833}{A^{2/3}}+0.794\frac{(N-Z)}{A}$
V_{LS}	$8.087-\frac{151.9}{A^2}+0.13(E-35)$	$+5.79\frac{(N-Z)}{A}-0.18\frac{Z}{A^{1/3}}$	$-5.79\frac{(N-Z)}{A}$
r_{LS}		$1.151-\frac{0.470}{A^{2/3}}$	$1.138-\frac{0.424}{A^{2/3}}$
a_{LS}		$0.418+\frac{0.548}{A^{2/3}}+0.335\frac{(N-Z)}{A}$	$0.423+\frac{0.627}{A^{2/3}}$

TABLE II. Optical-potential parameters for the set-2 potential.

		Proton	Neutron
V_0	$42.91+\frac{758.2}{A^2}-0.3(E-35)$	$+13.06\frac{(N-Z)}{A}+0.4\frac{Z}{A^{1/3}}$	$-13.06\frac{(N-Z)}{A}$
r_r		$1.184-\frac{0.906}{A^{2/3}}$	$1.806-\frac{1.048}{A^{2/3}}$
a_r		$0.742-\frac{0.584}{A^{2/3}}$	$0.742-\frac{0.584}{A^{2/3}}$
W_D	$3.364+0.01(E-35)$	$+5.00\frac{(N-Z)}{A}-0.01\frac{Z}{A^{1/3}}$	$-5.00\frac{(N-Z)}{A}$
r_i		$1.806-\frac{1.048}{A^{2/3}}$	$1.806-\frac{1.048}{A^{2/3}}$
a_i		$0.403+\frac{0.872}{A^{2/3}}$	$0.403+\frac{0.872}{A^{2/3}}$
V_{LS}	$8.087-\frac{151.9}{A^2}+0.13(E-35)$	$+5.79\frac{(N-Z)}{A}-0.18\frac{Z}{A^{1/3}}$	$-5.79\frac{(N-Z)}{A}$
r_{LS}		0.940	0.940
a_{LS}		0.491	0.491

sets as demonstrated in Fig. 2(b). Figure 2(c) shows a comparison of experimental neutron scattering cross sections (taken from Ref. [22]) with optical model cross sections calculated using the present potential parameter sets. The parameter set 2 will be used hereafter in the DWBA analysis of the $^{14}C(p,n)^{14}N$ reaction.

IV. ANALYSIS

The code DWBA-74 [33] was employed in the present microscopic DWBA analysis of the $^{14}C(p,n)^{14}N$ data. The optical-potential parameters were discussed in the previous section. The Cohen-Kurath (CK) [9] wave functions were used for the transitions to the positive-parity states. Those for the negative parity transitions were calculated with the Millener-Kurath interaction (MK) [10] assuming one-particle jump. Single-particle wave functions were generated in a Woods-Saxon-type bound-state potential with $r_0=1.25$ fm, $a=0.65$ fm, and $V_{LS}=6$ MeV, and the depth adjusted to reproduce the binding energy of a proton or a neutron.

The effective nucleon-nucleon interactions of Bertsch *et al.* [34] (M3Y) are used in the DWBA calculation. Results with other effective interactions, i.e., ones given by Anantaraman, Toki, and Bertsch [35], and by Hosaka, Kubo, and Toki [36], show no significant differences. The reliability of the information extracted from such DWBA analyses of the (p,n) data at 35 MeV has been discussed in detail in Ref. [11].

V. RESULTS AND DISCUSSION

It can be seen in the neutron excitation energy spectra illustrated in Figs. 1(a) and (b) that, in addition to strong peaks leading to the 3.947-MeV (1^+) and 8.48-MeV (4^-) states, there are relatively weak peaks corresponding to the 0.0 (1^+), 2.312 (0^+), 5.016 (2^-), 5.690 (1^-), 5.832 (3^-), and 7.026 (2^+) MeV states. The spins and parities of these states are well known and given in parentheses [37]. As seen in this list, the spectrum contains almost all samples of spin-isospin excitations, i.e., GT transition, $0^+\rightarrow 2^-$ transition, stretched-state excitations of $0\hbar\omega$ and $1\hbar\omega$ character, and others. We discuss each specific transition separately in this section.

A. $0^+\rightarrow 0^+$ and other natural-parity transitions

Figure 3(a) shows experimental and calculated angular distributions of neutrons leading to the 2.312-MeV 0^+ state. The data for this analog transition have been used to determine the optical-potential parameters as described in Sec. III. The solid curves in the figure are results of macroscopic DWBA calculations. Calculations with other optical-potential parameter sets give similar results as far as the forward-angle cross sections are concerned.

The shell-model predicts strong natural-parity transitions to the 5.690-MeV 1^-, 5.832-MeV 3^-, and 7.026-MeV 2^+ states. In the present experiment, these states have been observed with substantial strengths. Figures 3(b), 4(a), and 4(b) illustrate the angular distributions of differential cross sections leading to these states. Also shown are DWBA predictions calculated with spectroscopic amplitudes described previously. Normalization factors introduced to optimize DWBA fitting are given by N in the figures. Contrary to the cases in the $^{16}O(p,n)^{16}F$ reaction [11], the normalization factors for the 1^- and 3^- transitions in ^{14}C are more than unity. On the other hand, the normalization factor of 0.45 is needed for the 7.026-MeV (2^+) state. It has been found, as shown in Fig. 4(b), the 7.026-MeV state is also most dominantly excited by the $\Delta J(\Delta L,\Delta S)=2(2,1)$ component. It is interesting to note that the normalization factor of 0.45 obtained for the 7.026-MeV state is almost identical to those for the dominant 1(2,1) and 2(2,1) transitions in the $^{34}S(p,n)^{34}Cl$ reaction reported in Ref. [2].

B. $0^+\rightarrow 1^+$ transitions

There are two well-known $1^+, T=0$ states at 0.0 (g.s.) and 3.947 MeV in ^{14}N. A strong transition is expected to the 3.947-MeV 1^+ state based on shell-model predictions, although β decay to or from this state is not energetically possible. On the other hand, the ground-state transition

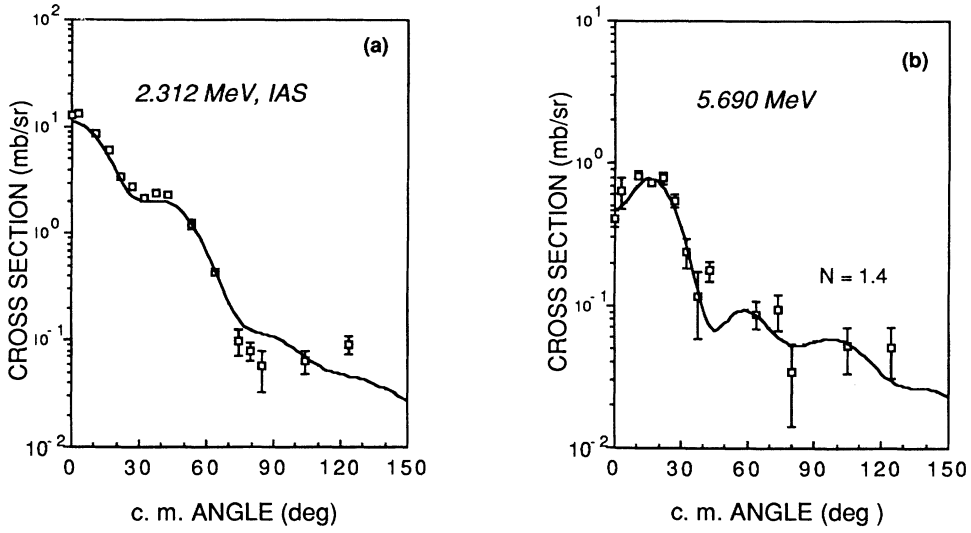

FIG. 3. (a) Differential cross sections for neutrons from the $^{14}C(p,n)^{14}N$ reaction leading to the 0^+ analog ground state at 2.312 MeV. Curves are the results of macroscopic DWBA calculations with optical-potential parameter set 2. (b) Differential cross sections for neutrons from the $^{14}C(p,n)^{14}N$ reaction leading to the 1^- state at 5.690 MeV. The curve is microscopic DWBA results. The normalization factor introduced to optimize the fitting is shown by N in the figure.

is equivalent to the forbidden β decay of ^{14}C, which has a logft value of 9.0, and the (p,n) strength should be highly suppressed if the proportionality between B(GT) and (p,n) cross section holds as mentioned in the introduction. In our previous reports [5], however, we have shown that a $\Delta J^{\pi}=1^+$ transition with small B(GT) sometimes has a considerable (p,n) strength through the $\Delta J(\Delta L,\Delta S)=1(2,1)$ channel which does not contribute to the B(GT) matrix element.

As seen in the neutron spectrum illustrated in Fig. 1(a), the (p,n) transition to the ground state is not highly suppressed. However, the dominant fraction of the $^{14}C(p,n)^{14}N$(g.s.) cross section can be attributed to the $L=2$ component in the transition. This is illustrated in Fig. 5, where the measured angular distribution is compared with the DWBA calculations for each $\Delta J(\Delta L,\Delta S)$ component and their sum. The angular distribution of neutrons leading to the ground state, shown in Fig. 5(a), is quite different from that of the dominant GT-type transition leading to the 3.947-MeV state and that leading to the high-lying $T=1$, 1^+ state shown in Figs. 6(a) and (b). The present DWBA calculations well reproduce these different angular distribution shapes, indicating that the dominant fraction of the (p,n) cross section for the ground state can be attributed to the 1(2,1) transition, while that for the 3.947-MeV state to the 1(0,1) GT type.

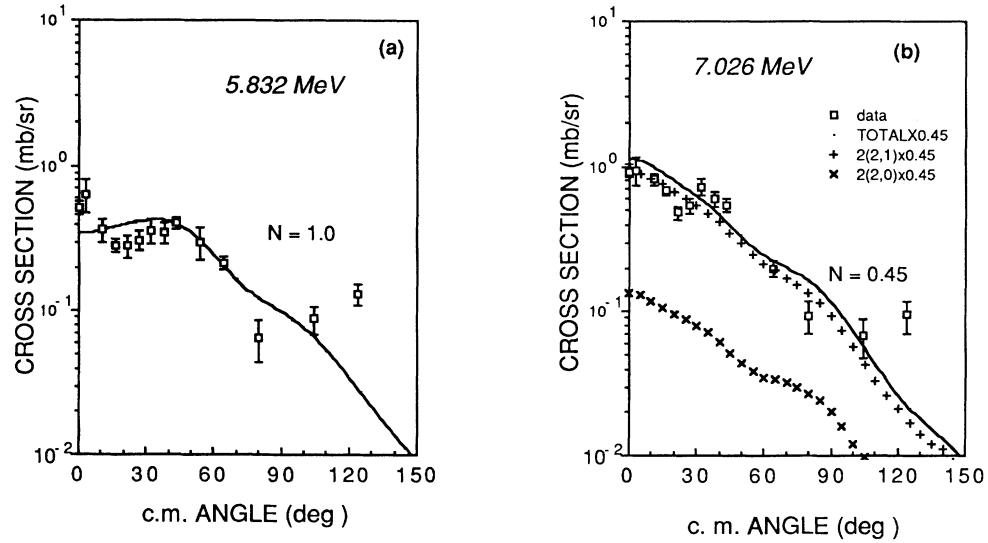

FIG. 4. Same as Fig. 3(b) but for the transitions leading to the 3^- state at (a) 5.832 MeV, and to the 2^+ state at (b) 7.026 MeV.

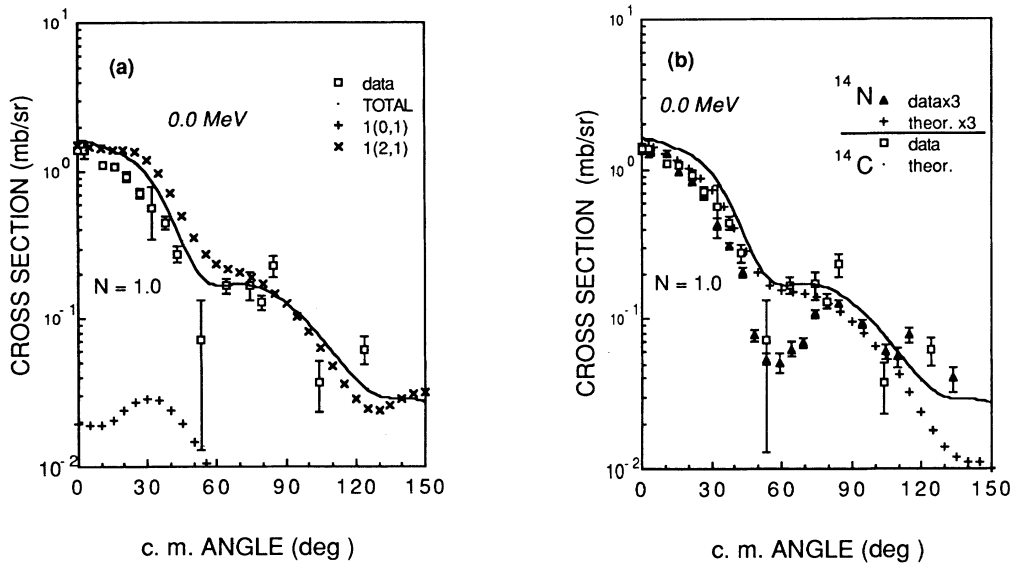

FIG. 5. (a) Differential cross sections for neutrons from the $^{14}C(p,n)^{14}N$ reaction leading to the 1^+ ground state. Contributions from $\Delta J(\Delta L,\Delta S)=1(0,1)$ and 1(2,1) components are shown separately. (b) Those for the $^{14}N(p,n)^{14}O$ reaction are illustrated together with those for the $^{14}C(p,n)^{14}N$ reaction for comparison. Experimental and calculated cross sections for the former are multiplied by the statistical spin and isospin coupling factor of 3.

The present result is in agreement with the hindered GT transition to the ground state. The shell-model GT strength for the ground state is not as fully canceled, however. The logft value obtained with the CK wave functions is 5.4, much smaller than the experimental value of 9.0. Accordingly the shell-model calculation predicts 1:300 for the cross-section ratio of the 1(0,1) component for the ground state to that for the 3.947-MeV state as seen in Figs. 5(a) and 6(a). The calculated (p,n) angular distribution for the ground state is insensitive to the magnitude of the 1(0,1) component since its contribution is very small as seen in Fig. 5(a).

In Fig. 5(b), cross sections for the $0^+ \rightarrow 1^+$ ground-state transition are compared with those for $1^+ \rightarrow 0^+$ transition in the $^{14}N(p,n)^{14}O$(g.s.) reaction. It is remarkable that these two are quite similar except for the absolute magnitudes of the cross section due to the statistical spin and isospin coupling factor of 3.

The normalization factor is close to unity for the ground-state transition, while it is ~ 0.5 for the GT transition to the 3.947-MeV state. The latter factor is similar to those obtained in intermediate-energy (p,n) reactions

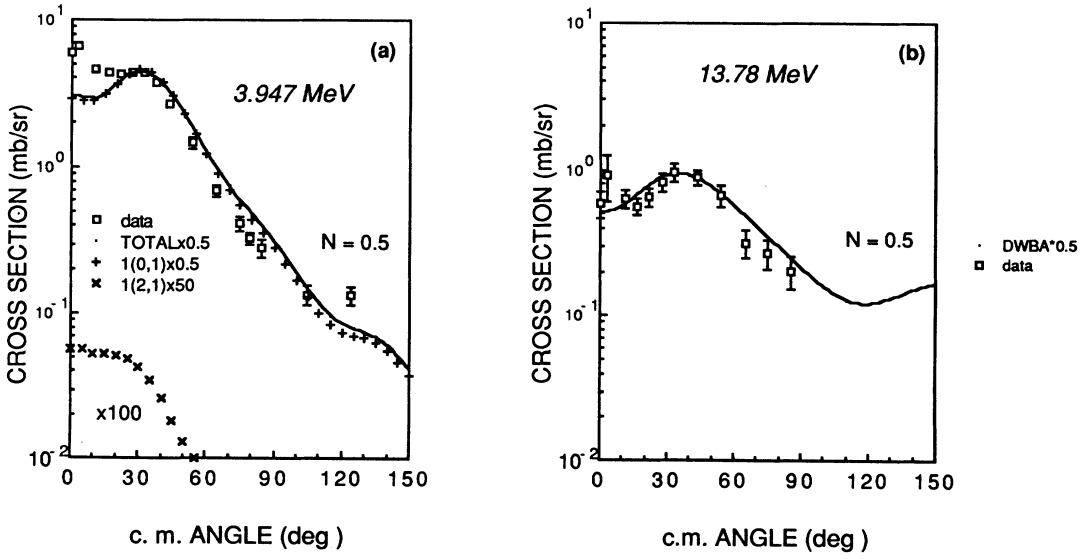

FIG. 6. Same as Fig. 3(b) but for the transitions leading to the 1^+ states at (a) $E_x = 3.947$ MeV and (b) 13.78 MeV. Contributions from $\Delta J(\Delta L,\Delta S)=1(0,1)$ and 1(2,1) components are shown separately for the 3.947 MeV state.

throughout the periodic table [38].

The $T=1$, 1^+ state at $E_x=13.78$ MeV, reported by Rapaport *et al.* [7] in their (p,n) work, is seen to be excited in Figs. 1(a) and (b). Its angular distribution is shown in Fig. 6(b) together with the DWBA calculation. The (p,n) intensity ratio of this transition to that for the 3.947-MeV state at the peak is 0.26, which is in good agreement with that estimated in the 0° neutron spectrum in Ref. [7].

C. Stretched-state transitions

A peak due to the 4^- state at 8.48 MeV in ^{14}N dominates over other peaks in the backward-angle neutron spectrum shown in Fig. 1(b), where neutron yields for high-spin state are relatively enhanced. Another state to be remarked on is the 3^+ state at 6.444 MeV, although it is weakly populated at these angles of Figs. 1(a) and (b). The former corresponds to the $1\hbar\omega$ stretched particle-hole state with the configuration $(\pi d_{5/2}, \nu p_{3/2}^{-1})_{4^-}$, and the latter to the $0\hbar\omega$ stretched excitation $(\pi p_{3/2}, \nu p_{3/2}^{-1})_{3^+}$.

A stretched particle-hole state is thought to be of particular interest because of its simple and pure wave function, and has been extensively studied with a variety of probes such as charge-exchange reaction, proton and electron scattering. It has been found that we need surprisingly small normalization factors for $1\hbar\omega$ stretched-state excitations. The experimental cross sections are only about 30% of the predictions calculated with pure configurations [39], independently of the probe or of the projectile energy. Recent studies revealed [40] that in many cases the $1\hbar\omega$ stretched-strength spreads over several states, while almost full $0\hbar\omega$ strength is concentrated in a single low-lying state, for which reasonable spectroscopic amplitudes are available based on shell-model wave functions. These altogether lead to a conclusion that the large quenching observed in $1\hbar\omega$ transitions seems to be due to complicated configuration mixing, as discussed by Amusa and Lawson [41] and by Carr *et al.* [42], against the original expectation.

The angular distributions of neutrons leading to the $0\hbar\omega$ 3^+ and $1\hbar\omega$ 4^- stretched states are shown in Figs. 7(a) and (b), respectively, along with the DWBA results. The experimental cross sections for the $0^+\rightarrow 3^+$ transition are almost absolutely fitted by the calculation, while the measured $0^+\rightarrow 4^-$ transition is enhanced ($N=1.6$). The discrepancy between the experiment and calculation in the latter case is much larger than the uncertainty in the experimental absolute cross sections. The source of discrepancy can hardly be attributed to the uncertainty in the isovector part of the tensor interaction of the effective nucleon-nucleon interaction, since the same interaction was found [1] to describe very well the $\Delta J^\pi=0^-$ transitions in p-shell nuclei in the region of momentum transfer $q<1.3$ fm^{-1}.

D. Other unnatural-parity transitions

The most important sample of this group may be the $0^+\rightarrow 0^-$ transition, which can be an important probe of the pure longitudinal spin response. Unfortunately, the present target was too thin to observe this weakly populated peak with sufficient statistical accuracies over a wide range of angles.

Figure 8 illustrates the experimental and theoretical differential cross sections for the $0^+\rightarrow 2^-$ transition to the 5.016-MeV, $T=0$ state. A satisfactory fit was obtained with a normalization factor of 0.8. The 2^- excitations observed in the (p,n) reactions on ^{12}C and ^{16}O were previously reported in Ref. [11]. The cross sections of the 2^- transition in ^{12}C were fitted absolutely, while a normalization factor of 0.5 was required for that in ^{16}O. The dominant shell-model configurations for the former reaction are $(\pi 2s_{1/2}, \nu 1p_{3/2}^{-1})$ and $(\pi 1d_{5/2}, \nu 1p_{3/2}^{-1})$ (they con-

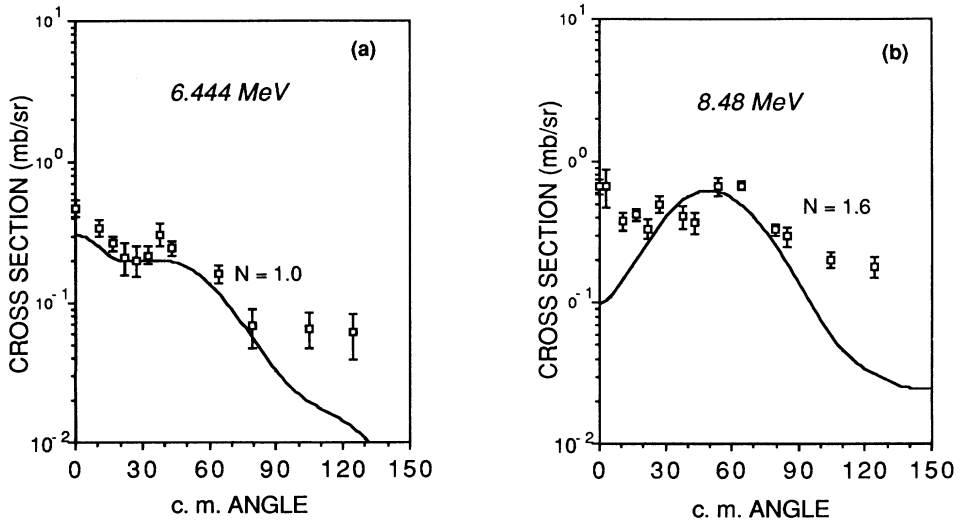

FIG. 7. Same as Fig. 3(b) but for the 3^+ state at (a) 6.444 MeV, and for the 4^- state at (b) 8.48 MeV.

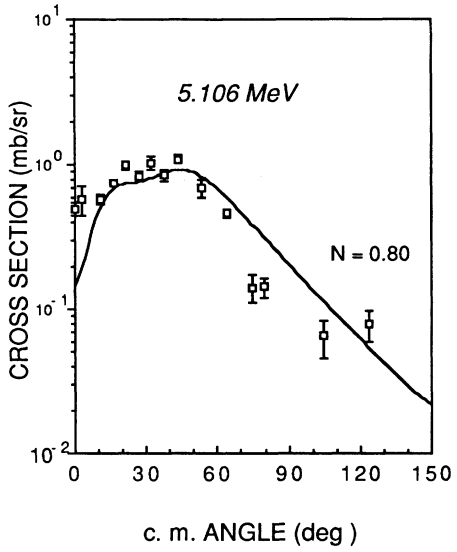

FIG. 8. Same as Fig. 3(b) but for the 2^- state at 5.016 MeV.

tribute constructively to cross sections), and that for the latter is $(\pi 1d_{5/2}, \nu 1p_{1/2}^{-1})$. The normalization factor for the 2^- transition in ^{14}C is close to unity, although the dominant configuration is $(\pi 1d_{5/2}, \nu 1p_{1/2}^{-1})$.

VI. SUMMARY

We have studied the $^{14}C(p,n)^{14}N$ reaction at $E_p=35$ MeV. Comprehensive sets of optical-potential parameters have been derived in the course of the analysis. A number of spin-isospin excitations were observed along with isovector natural-parity transitions. A normalization factor of ~ 0.5 was needed to fit the cross sections for the strong 1^+ transition to the 3.947-MeV state. A similar factor was obtained for the 2^+ transition to the 7.026-MeV state, whose dominant component is $\Delta J(\Delta L,\Delta S)=2(2,1)$. The cross sections for the other transitions were well accounted for by the shell-model transition amplitudes, except for the $1\hbar\omega$ 4^- stretched-state excitation where a slight enhancement was observed.

ACKNOWLEDGMENTS

The authors are indebted to Prof. B. A. Brown and Prof. K. Muto for their help in the calculation of spectroscopic amplitudes. They appreciate the help of Prof. C. D. Zafiratos for preparation of the target. This work was partly supported by a Grant-in-Aid for Scientific Research, No. 59540147, from the Ministry of Education.

[1] H. Orihara, M. Kabasawa, K. Furukawa, T. Kawamura, Y. Takahashi, A. Satoh, T. Niizeki, T. Nakagawa, K. Maeda, K. Ishii, K. Miura, and H. Ohnuma, Phys. Lett. **187**, 240 (1987).

[2] K. Furukawa, M. Kabasawa, T. Kawamura, Y. Takahashi, A. Satoh, T. Nakagawa, H. Orihara, T. Niizeki, K. Ishii, K. Maeda, K. Miura, B. A. Brown, and H. Ohnuma, Phys. Rev. C **36**, 1686 (1987).

[3] H. Orihara, S. Nishihara, T. Murakami, K. Maeda, K. Furukawa, T. Nakagawa, G. C. Kiang, K. Miura, and H. Ohnuma, Phys. Rev. Lett. **48**, 469 (1982).

[4] H. Orihara, S. Nishihara, K. Furukawa, T. Nakagawa, K. Maeda, K. Miura, and H. Ohnuma, Phys. Rev. Lett. **49**, 1318 (1982).

[5] T. N. Taddeucci, C. A. Goulding, T. A. Carey, R. C. Byrd, C. D. Goodman, C. Gaarde, J. Larsen, D. Horen, J. Rapaport, and E. Sugarbaker, Nucl. Phys. **A469**, 125 (1987).

[6] See, for example, T. N. Taddeucci, R. R. Doering, A. Galonsky, and S. M. Austin, Phys. Rev. C **29**, 764 (1984).

[7] J. Rapaport, D. Wang, J. A. Carr, F. Petrovich, C. C. Foster, C. D. Goodman, C. Gaarde, J. Larsen, C. A. Goulding, T. N. Taddeucci, D. Horen, and E. Sugarbaker, Phys. Rev. C **36**, 500 (1987).

[8] E. Sugarbaker, D. Marchlenski, T. N. Taddeucci, L. J. Rybarcyk, J. B. McClelland, T. A. Carey, R. C. Byrd, C. D. Goodman, W. Huang, J. Rapaport, D. Mercer, D. Prout, W. P. Alford, E. Gülmez, C. A. Whitten, and D. Ciskowski, Phys. Rev. Lett. **65**, 551 (1990).

[9] S. Cohen and D. Kurath, Nucl. Phys. **A101**, 1 (1967).

[10] D. J. Millener and D. Kurath, Nucl. Phys. **A255**, 315 (1975).

[11] H. Ohnuma, M. Kabasawa, K. Furukawa, T. Kawamura, Y. Takahashi, A. Satoh, T. Nakagawa, K. Maeda, K. Miura, T. Niizeki, and H. Orihara, Nucl. Phys. **A467**, 61 (1987).

[12] H. Orihara, S. Nishihara, K. Furukawa, M. Kabasawa, T. Kawamura, Y. Takahashi, T. Nakagawa, and K. Maeda, Nucl. Instrum. Methods **A257**, 189 (1987).

[13] W. D. Myers, Nucl. Phys. **A204**, 465 (1973).

[14] E. F. Fabrici, S. Micheletti, M. Pignanelli, F. G. Resmini, R. De Leo, G. D'Erasmo, A. Pantaleo, J. L. Escudie, and A. Tarrats, Phys. Rev. C **21**, 844 (1980).

[15] F. D. Becchetti, Jr. and G. W. Greenlees, Phys. Rev. **182**, 1190 (1969).

[16] J. D. Carlson, C. D. Zafiratos, and D. A. Lind, Nucl. Phys. **A249**, 29 (1975).

[17] G. J. Pyle, University of Minnesota Report No. C00-1265-64 (unpublished).

[18] A parameter search code for elastic and quasielastic scattering. Quasielastic calculations are made using the Lane model and adopted from the code DWUCK4 by P. D. Kunz.

[19] H. Ohnuma, B. A. Brown, D. Dehnhard, K. Furukawa, T. Hasegawa, S. Hayakawa, N. Hoshino, K. Ieki, M. Kabasawa, K. Maeda, K. Miura, K. Muto, T. Nakagawa, K. Nisimura, H. Orihara, T. Suehiro, T. Tohei, and M. Yasue, Nucl. Phys. **A456**, 61 (1986).

[20] H. Ohnuma, N. Hoshino, K. Ieki, M. Iwase, H. Shimizu,

H. Toyokawa, T. Hasegawa, K. Nisimura, M. Yasue, M. Kabasawa, T. Nakagawa, T. Tohei, H. Orihara, S. I. Hayakawa, K. Miura, T. Suehiro, S. K. Nanda, D. Dehnhard, and M. A. Franey, Nucl. Phys. **A514**, 273 (1990); (unpublished).

[21] K. Ieki, J. Iimura, M. Iwase, H. Ohnuma, H. Shimizu, H. Toyokawa, K. Furukawa, M. Kabasawa, T. Nakagawa, T. Tohei, H. Orihara, S. I. Hayakawa, T. Hasegawa, K. Nisimura, M. Yasue, K. Miura, T. Suehiro, and M. A. Franey, Phys. Rev. C **42**, 457 (1990); (unpublished).

[22] J. S. Petler, M. S. Islam, R. W. Finlay, and F. S. Dietrich, Phys. Rev. C **32**, 673 (1985).

[23] P. Grabmayer, J. Rapaport, and R. W. Finlay, Nucl. Phys. **A350**, 167 (1980).

[24] D. G. Montague, R. K. Cole, P. S. Lewis, and C. N. Waddell, Nucl. Phys. **A199**, 433 (1973).

[25] O. Karban, J. Lowe, P. D. Greaves, and V. Hnizdo, Nucl. Phys. **A133**, 255 (1969).

[26] R. De Leo, G. D'Erasmo, A. Pantaleo, M. N. Harakeh, E. Cereda, S. Micheletti, and M. Pignanelli, Phys. Rev. C **28**, 1443 (1983).

[27] O. Karban, P. D. Greaves, V. Hnizdo, J. Lowe, N. Berovic, Wojciechowski, and G. W. Greenlees, Nucl. Phys. **A132**, 548 (1969).

[28] L. F. Hansen, F. S. Dietrich, B. A. Pohl, C. H. Poppe, and C. Wong, Phys. Rev. C **31**, 111 (1985).

[29] R. C. Byrd, C. E. Floyd, K. Murphy, P. P. Guss, and R. L. Walter, Nucl. Phys. **A427**, 36 (1984).

[30] K. Gul, M. Anwar, M. Ahmad, S. m. Saleem, and Naeem A. Khan, Phys. Rev. C **24**, 2458 (1981).

[31] E. Woye, W. Tornow, G. Mack, C. E. Floyd, P. P. Guss, K. Murphy, R. C. Byrd, S. A. Wender, R. L. Walter, T. B. Clegg, and W. Wylie, Nucl. Phys. **A394**, 139 (1983).

[32] S. T. Lam, W. K. Dawson, S. A. Elbakr, H. W. Fielding, P. W. Green, R. L. Hermer, I. J. van Heerden, A. H. Hussein, S. P. Kwan, G. C. Neilson, T. Otsubo, D. m. Sheppard, H. s. Sherif, and J. Soukup, Phys. Rev. C **32**, 76 (1985).

[33] R. Schaeffer and J. Raynal, Centre d'Etude Nucleaires de Saclay Report CEA-R4000 (1970).

[34] G. Bertsch, J. Borysowicz, H. McManus, and W. G. Love, Nucl. Phys. **A284**, 399 (1977).

[35] N. Anantaraman, H. Toki, and G. Bertsch, Nucl. Phys. **A398**, 269 (1983).

[36] A. Hosaka, K.-I. Kubo, and H. Toki, Nucl. Phys. **A444**, 76 (1985).

[37] F. Ajzenberg-Selove, Nucl. Phys. **A360**, 1 (1981).

[38] C. Gaarde *et al.*, in *Spin Excitation in Nuclei,* edited by F. Petrovich *et al.* (Plenum, New York, 1984), p. 65.

[39] R. A. Lindgren and F. Petrovich, in *Spin Excitation in Nuclei,* edited by F. Petrovich *et al.* (Plenum, New York, 1984), p. 323.

[40] See, for example, R. J. Peterson, M. Yasue, M. H. Tanaka, T. Hasegawa, N. Nisimura, H. Ohnuma, H. Shimizu, K. Ieki, H. Toyokawa, M. Iwase, J. Iimura, and S. I. Hayakawa, Phys. Rev. C **38**, 1130 (1988).

[41] A. Amusa and R. D. Lawson, Phys. Rev. Lett. **51**, 103 (1983).

[42] J. A. Carr, S. D. Bloom, F. Petrovich, and R. J. Philpot, Phys. Rev. Lett. **62**, 2249 (1989).